Improving Long-Range RTK
Getting a Better Handle on the Biases

Don Kim and Richard B. Langley

SCIENTISTS AND ENGINEERS continue to improve high-accuracy GPS positioning techniques — techniques pioneered a quarter of a century ago. The first GPS satellite, SVN01/PRN04, was launched from Cape Canaveral on February 22, 1978. And between 1978 and 1985, the U.S. Air Force orbited nine more prototype or Block I satellites to test key technologies before deploying the operational constellation.

Surveyors and geodesists were among the earliest users of the Block I satellites. Using the satellite signals, they developed accurate positioning techniques based on the use of carrier-phase observations — about two orders of magnitude more precise than code measurements. To reduce the effect of biases and errors in the measurements, they developed the concepts of between-satellite and between-receiver single differencing of the carrier-phase data as well as double and triple differencing. Raw measurements were recorded by receivers and then post-processed to obtain receiver coordinates. Clever approaches were developed to handle the integer ambiguity of the carrier phases.

With the launch of the Block II satellites beginning in 1989, further improvements in positioning accuracy and efficiency became possible, including real-time carrier-phase-based positioning with a radio link between a reference receiver and a remote receiver. This technique became known as real-time kinematic or RTK, as it permitted the remote receiver to rove and occupy different points in a single positioning exercise. But carrier-phase ambiguity resolution issues coupled with inaccurately modeled satellite orbit and atmospheric effects has limited consistent single-baseline RTK operation between reference and rover receivers to tens of kilometers. On longer baselines, inaccurate modeling can result in significant positioning errors. Network RTK, using simultaneously operating reference stations to better determine error corrections, can extend the area of coverage of RTK but it, too, has limitations.

In this month's column, I am joined by my colleague Don Kim who has developed an innovative approach to long-range RTK. We describe how accurate modeling of atmospheric effects coupled with an ionosphere-free ambiguity resolution process results in successful long-range RTK that can be implemented in either single-baseline or network mode. Has the ultimate RTK approach been developed? Probably not. But we're getting closer.

"Innovation" is a regular column that features discussions about recent advances in GPS technology and its applications as well as the fundamentals of GPS positioning. The column is coordinated by Richard Langley of the Department of Geodesy and Geomatics Engineering at the University of New Brunswick, who welcomes your comments and topic ideas. To contact him, see the "Contributing Editors" section on page 6.

INNOVATION INSIGHTS
with Richard Langley

Has the ultimate RTK approach been developed?

Biases and errors such as satellite orbit error and atmospheric signal refraction are the primary limiting factors in successful long-baseline, real-time kinematic (RTK) style processing of GPS measurements — either in real-time or post-processing mode. These error sources are dependent on the distance between a reference and rover receivers. If they are not adequately accounted for, they can result in significant positioning errors in long-baseline applications. This is particularly true for the conventional single-baseline RTK and hence reduces the effective inter-receiver distance of this technique to a few tens of kilometers.

We can apply effective strategies to mitigate these error sources. For example, the ionosphere-free linear combination of the L1 and L2 carrier-phase measurements can completely cancel first-order ionospheric delays. Although this approach is appealing for mitigating the ionospheric errors, we have to be prepared to accept some penalty. As it is difficult to fix integer ambiguities using the ionosphere-free observations for long baselines, float ambiguity solutions (less accurate than fixed ones) are normally used. Due to the amplification of the noise by the linear combination, the solutions are less precise. Errors in broadcast GPS satellite orbits have little effect for baselines up to a few hundred kilometers and, furthermore, can be virtually eliminated using precise ephemerides in post-processing mode. Tropospheric delay is usually estimated based on model atmospheric predictions and/or surface meteorological observations made near the stations at the time of the GPS measurements. As this approach often inappropriately accounts for spatial and temporal variations in water vapor delays, it is a common procedure to estimate a

residual zenith delay from the data itself.

As an alternative approach to mitigating the error sources, network RTK based on multiple reference stations is often used. The integration of several reference stations into a combined network provides a capability for modeling the error sources at a rover within the network and enables lengthening the baselines up to a few hundreds of kilometers. Despite successful implementation of network RTK for long-baseline applications, however, its performance is not always equivalent to single-baseline RTK operating in short-baseline situations. As network RTK interpolates error corrections for a rover using the error estimates at reference stations, this approach is vulnerable to localized anomalous errors under unfavorable atmospheric conditions. For example, weather fronts and atmospheric conditions associated with heavy rainfall can cause rapid variations in the tropospheric delay and, subsequently, the performance of an RTK system can be significantly degraded even across relatively short baselines. Such anomalies are not canceled in the interpolation procedure used for deriving rover delays. Also, solar-terrestrial interactions can cause significant changes in the morphology of the ionosphere, changing the propagation delay of GPS signals within time intervals as short as one minute. Such changes can last for several hours primarily in the polar, auroral, and equatorial ionospheres. During severe ionospheric activity, the correction accuracy deteriorates and adversely affects the ambiguity resolution over the network. When a rover is located outside the network boundary, network RTK must extrapolate error corrections for the rover. As a result, network RTK can face the same challenges as single-baseline RTK.

Over the past few years, University of New Brunswick (UNB) researchers have carried out several projects involving long baselines that, unfortunately, could not take advantage of network RTK. These included a field experiment to investigate the performance of different neutral atmosphere mitigation strategies during the 2005 mission of the Canadian Coast Guard Ship Amundsen (a research icebreaker) in the Canadian Arctic and Hudson Bay, and collaboration with the University of Southern Mississippi to advance positioning results by means of improved differential tropospheric modeling in the marine environment of the Bay of Fundy in eastern Canada. In both studies, the number of reference stations deployed was not sufficient to adequately model the errors using network RTK. Instead, our approach for achieving high accuracies at greater distances from differential reference stations was to use single-baseline RTK in a novel post-processing mode.

In this article, we describe our new approach for long-range RTK. Although this approach was originally developed for single-baseline RTK over long distances in kinematic mode, it can be used for network RTK when requiring extrapolation of the differential ionosphere corrections for a rover located outside the network. It can also be used in cases where the rover located inside the network is experiencing local anomalies in the differential ionospheric delays.

New Approach Considerations

The most common approach for achieving high accuracies with GPS technology in kinematic situations is RTK-style processing. On designing an appropriate approach for long-range (say, 30–100 kilometers) single-baseline RTK, we consider two basic requirements. Firstly, our new approach will be used in real-time applications such as machine guidance and vehicle navigation. More specifically, single epoch carrier-phase observations will be used to resolve ambiguities (that is, an epoch-by-epoch ambiguity resolution) in real-time situations. Secondly, the new approach will provide positioning solutions using fixed ambiguities rather than the ionosphere-free float ambiguities.

The Observation Model. In our approach, we use carrier-phase observations double-differenced between satellites and receivers (DD). The linearized GPS carrier-phase observation model for long-range single-baseline applications is given as:

$$\mathbf{y}_i = \mathbf{A}\mathbf{x} + \mathbf{s} + \mathbf{T} - \mathbf{I}_i + \lambda_i \mathbf{N}_i + \mathbf{e}_i, \, Cov[\mathbf{e}_i] = \mathbf{Q}_{\mathbf{y}_i}, \, i = 1 \text{ or } 2, \qquad (1)$$

where $\mathbf{y}$ is the vector of DD carrier-phase observations in distance units; $\mathbf{x}$ is the vector of unknown baseline components; $\mathbf{s}$ is the vector of orbit error contributions to the DD carrier-phase observations; $\mathbf{T}$ is the vector of DD tropospheric delays; $\mathbf{I}$ is the DD ionospheric delay parameter vector where $\mathbf{I}_2 = (f_{L1}^2/f_{L2}^2)\mathbf{I}_1$; $\mathbf{A}$ is the design matrix corresponding to $\mathbf{x}$; $\mathbf{N}$ is the vector of DD ambiguities; f and λ are the frequency and wavelength of the carrier-phase observations, respectively; $\mathbf{e}$ is the noise vector including multipath, residual ionospheric delay (higher-order ionospheric effects and ionospheric scintillation) and receiver system noise; $Cov[\cdot]$ represents the variance-covariance operator; $\mathbf{Q}_\mathbf{y}$ is the variance-covariance matrix of the observations; and i indicates the L1 or L2 signal.

The Objective Function. Least-squares estimation with integer constraint for the ambiguity parameters is referred to as an integer least-squares problem. The objective function to be minimized in the integer least-squares problem, Ω, is given as:
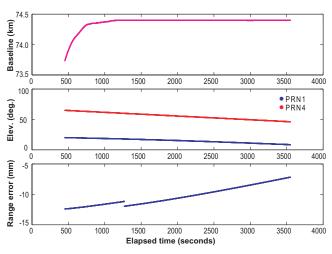
$$\Omega_i = \left(\hat{\mathbf{N}}_i - \check{\mathbf{N}}_i\right)^T \mathbf{Q}_{\hat{\mathbf{N}}_i}^{-1} \left(\hat{\mathbf{N}}_i - \check{\mathbf{N}}_i\right), \, with \, \check{\mathbf{N}}_i \in \mathbf{Z}^n, \, i = 1 \text{ or } 2, \qquad (2)$$

where $\hat{\mathbf{N}}$ is the vector of float ambiguity estimates; $\check{\mathbf{N}}$ is the vector of integer ambiguity candidates selected in the ambiguity search process; $\mathbf{Q}_{\hat{\mathbf{N}}}$ is the variance-covariance matrix of the float ambiguity estimates; $\mathbf{Z}$ is the set of integers; n is the number of the observations; and, again, i indicates the L1 or L2 signal. We'll come back to the objective function, but let's examine the error sources first.

Satellite Orbit Errors. Errors in broadcast GPS satellite orbits have little effect for baselines up to a few hundred kilometers and, furthermore, can be virtually eliminated using precise ephemerides in post-processing mode. If we assume that the broadcast orbits have a worst-case accuracy of 4 meters (on average, they are actually better than this), the approximate baseline component error becomes around 2 centimeters for a 100-kilometer baseline.

We validated this "rule of thumb" calculation by comparing broadcast orbits to those of the National Geospatial-intelligence Agency (NGA), which provides precise GPS ephemeris files refer-

▲ **FIGURE 1** Double-differenced broadcast orbit errors based on a comparison with a precise ephemeris for the long baselines, projected onto the range directions

enced to satellite antenna phase center (APC) just like the broadcast orbits. **FIGURE 1** shows an example of double-differenced broadcast orbit errors compared to the NGA APC precise ephemeris for long baselines. These orbit errors were projected onto the range directions. The top panel shows the distances (about 74 kilometers) between a base station and a rover, the middle panel shows the elevation angles of the paired satellites used in double differencing, and the bottom panel shows the broadcast orbit errors in the range direction. The jump in the range-error plot is due to a switch in two-hour broadcast ephemeris sets. It is obvious that range-error differences using the broadcast orbit can reach up to a few centimeters for long baselines. But compared to the wavelength of the carrier-phase observations, range errors due to the broadcast orbits are not significant. This analysis confirms that we can safely ignore the orbit error term **s** in Equation (1) when using the broadcast orbits in real-time applications over a baseline of up to 100 kilometers in length.

Ionospheric Delays. The ionosphere-free linear combination and ionosphere modeling as a state both work well for long baselines once the parameter (ionospheric delay or float ambiguity) converges although it takes typically a few hours. In real-time applications requiring millimeter accuracy, however, these approaches are not practical. Instead, we use the ionosphere-nullification technique that instantaneously nullifies the effect of the differential ionospheric delay in an ambiguity search process.

In our technique, we combine the two independent L1 and L2 ambiguity search processes into one simultaneous ambiguity search process. When a pair of L1 and L2 ambiguity candidates is selected in the simultaneous search process, we can virtually eliminate the large residual ionospheric effects (the first-order differential ionospheric delays). Furthermore, this approach is able to instantaneously eliminate the differential ionospheric delay.

As the ionosphere-nullification technique estimates the ionospheric delays and ambiguities simultaneously using single-epoch carrier-phase observations (that is, an epoch-by-epoch ambiguity resolution), this technique may be less reliable than alternatives that model the ionospheric delays as a state in a Kalman filter or a sequential least-squares estimator. This is more likely to be true especially when the number of satellites being observed is insufficient (six or fewer satellites). However, under typical conditions (more than six satellites), the performance of the ionosphere-nullification technique is comparable to the alternatives.

Tropospheric Delays. In precise applications requiring millimeter accuracy, the tropospheric delay can be estimated by a simple parameterization of the tropospheric delay. The line of sight delay, D, is expressed as a function of four parameters as follows:

$$D = m_h(el)D_{hz} + m_w(el)D_{wz} + m_g(el)\left[G_N \cos(az) + G_E \sin(az)\right] \quad (3)$$

where D_{hz} is the zenith hydrostatic delay; D_{wz} is the zenith non-hydrostatic or (predominantly) wet delay; G_N and G_E are the north and east delay gradient in distance units, respectively; m_h, m_w, and m_g are the hydrostatic, wet, and gradient mapping functions, respectively; el is the non-refracted elevation angle at which the signal is received; and az is the azimuth angle at which the signal is received, measured east of north.

Under typical atmospheric conditions, GPS data may not have the sensitivity to detect atmospheric gradients and azimuthal asymmetry. In such a case, the tropospheric delay can be estimated by restricting the residual error to the zenith delay components.

In our technique, we use standard models for the *a priori* zenith hydrostatic delay, hydrostatic and wet mapping functions, and the gradient mapping function.

Estimation Model

Assuming that accurate real-time meteorological data are available at a reference station and a rover, we can almost perfectly account for the hydrostatic delay. And to avoid a mathematical correlation between the partial derivatives of the tropospheric delay at two stations, the levering technique can be used, which fixes the tropospheric delay at the reference station and estimates the relative delay at the rover. We can now form a new carrier-phase observation model to estimate the unknown parameters (that is, the baseline components, **x**, and the tropospheric delay, **T**) at every epoch. The ionospheric delay **I** and ambiguities **N** are resolved in the ambiguity search process using the ionosphere-nullification technique.
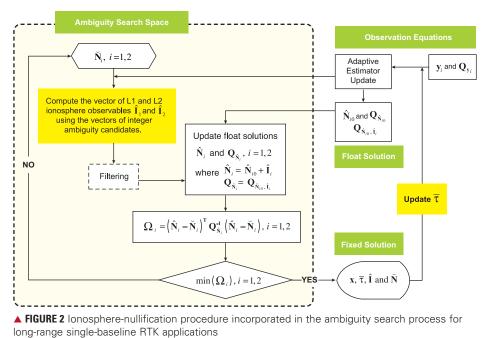
Adaptive Estimator. Since the tropospheric delays will not change dramatically under typical atmospheric conditions over a short time period, it might be better to estimate the tropospheric delay parameter adaptively as:

$$\bar{\tau}_k = \alpha\hat{\tau}_k + (1-\alpha)\bar{\tau}_{k-1}, 0 < \alpha \leq 1 \quad (4)$$

where $\hat{\tau}_k$ is the estimate of the tropospheric delay parameter at epoch k; $\bar{\tau}_k$ is the adaptive estimate of $\hat{\tau}_k$; and α is a "forgetting factor" which is reciprocal to a correlation time (i.e., a smoothing time interval). Depending on atmospheric conditions, we

can control the correlation time of the tropospheric delay parameter by changing α. We can initialize the procedure using $\overline{\tau}_0 = \hat{\tau}_0$, where $\hat{\tau}_0$ is an estimate of the tropospheric delay parameter at an initial epoch.

Ionosphere Nullification. Assuming that a simultaneous search process for the L1 and L2 ambiguity parameters has been established, a pair of L1 and L2 ambiguity candidates can be selected in the process. Then, we can derive the L1 and L2 ionosphere observables using the ambiguity candidates. As a matter of fact, each ambiguity candidate provides its corresponding ionosphere observation. Once we have a new ionosphere observation, we can estimate a new

▲ **FIGURE 2** Ionosphere-nullification procedure incorporated in the ambiguity search process for long-range single-baseline RTK applications

float ambiguity estimate, $\hat{\mathbf{N}}_i$. This new float ambiguity estimate is virtually free from the effects of the ionospheric delay. It should be noted that the updated variance-covariance matrix, $\mathbf{Q}_{\hat{\mathbf{N}}_i}(=\mathbf{Q}_{\hat{\mathbf{N}}_{i0},\hat{\mathbf{i}}_i})$, as well as the float solutions, $\hat{\mathbf{N}}_{i0}$ and $\mathbf{Q}_{\hat{\mathbf{N}}_{i0}}$, are computed once for every epoch's observations outside the ambiguity search space. We have to carry out the same procedure on each candidate sequentially until no ambiguity 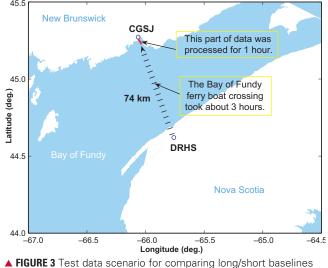candidate remains. Then, our goal is to find the ambiguity candidate that minimizes the objective function in Equation (2). **FIGURE 2** shows the ionosphere-nullification procedure.

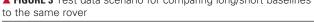One issue involved with the ionosphere-nullification technique is that the ionosphere observables are apt to be affected by multipath, receiver system noise, and residual ionospheric delay. As tropospheric delay and satellite orbit error are eliminated, they are irrelevant to the ionosphere observables.

It should be noted that multipath is normally a dominant error source in the ionosphere observables. So ideally, a GPS antenna should be installed in a clear place with no close-by reflector in the vicinity of the antenna if the ionosphere-nullification technique is to be used in RTK processing. Otherwise, we need to reduce the effects of multipath in the carrier-phase observations when we process the data. The "filtering" block in Figure 2 can be designed to help take care of this issue.
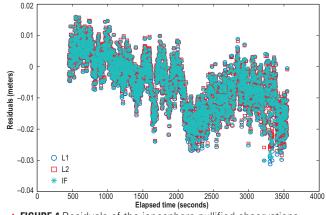
Test Results

We tested our approach using data from the Bay of Fundy field experiment. Two GPS reference stations had been deployed at the Canadian Coast Guard building in Saint John, New Brunswick (CGSJ), and at Digby Regional High School in Digby, Nova Scotia (DRHS), on either side of the Bay of Fundy near the terminals of an approximately 74-kilometer-long marine ferry route (see **FIGURE 3**). Two geodetic-grade receivers had been previously in-

▲ **FIGURE 3** Test data scenario for comparing long/short baselines to the same rover
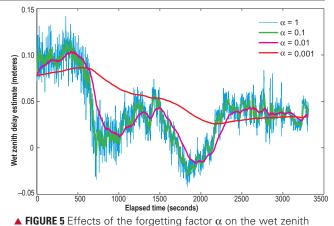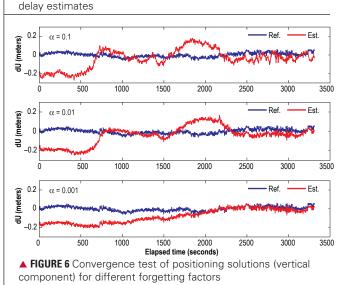
stalled at the reference stations and on the Princess of Acadia ferry. Surface meteorological equipment had also been collocated with the three receivers. This ferry repeats the same routes between two and four times daily, depending on the season. The Bay of Fundy is in a temperate climate region with significant seasonal tropospheric variations (with temperatures between -30°C and +30°C). Data had been collected over the course of one year from the daily ferry runs.

Using the UNB RTK software, we post-processed the data recorded at a 1 Hz data rate at the pair of base stations (CGSJ and DRHS) and the ferryboat on May 21, 2004. We used a zero elevation cutoff angle for data processing. One of the tools we use to assess the success of atmospheric modeling or other approaches, such as the ionosphere-nullification technique, is the comparison

▲ **FIGURE 4** Residuals of the ionosphere-nullified observations after fixing ambiguities

▲ **FIGURE 5** Effects of the forgetting factor α on the wet zenith delay estimates

▲ **FIGURE 6** Convergence test of positioning solutions (vertical component) for different forgetting factors

between short baseline (less than a few tens of kilometers) RTK solutions (for which RTK is generally regarded as reliable and uncontaminated by differential atmospheric uncertainties) and simultaneous position solutions from longer RTK baselines over which the atmospheric models or other approaches are being assessed. As we intended to compare long/short baselines to the same rover to

characterize long-baseline positioning performance, we processed a subset of the data near the end of a ferry run that provides such long/short baselines. Figure 3 illustrates the ferry crossing from Digby to Saint John and the data subset used. This arrangement provided both short (less than 3 kilometers) and long (greater than 73 kilometers) baselines at the same time for one hour.

Ionosphere Nullification. We obtained epoch-by-epoch estimates of the DD ionospheric delays using the ionosphere-nullification technique incorporated in the ambiguity resolution process. How do we know that the ionospheric delays in the L1 and L2 carrier-phase measurements are eliminated by the ionosphere-nullification technique? We can confirm this by examining the residual error in each observation.
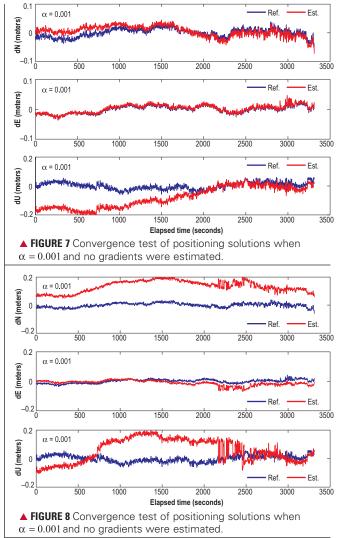
FIGURE 4 shows that the residuals of the L1 and L2 observations are almost identical to those of the ionosphere-free linear combinations. This implies that the effects of the ionospheric delays have been successfully nullified in the L1 and L2 observations. Minor differences in the residuals of the three observation types come from the noise models used for least-squares estimation. For simplicity, we did not propagate the uncertainty of the ionospheric delay estimates into the ionosphere-nullified L1 and L2 observations. The effects of this negligence are insignificant, as seen in Figure 4.

Tropospheric Delay Estimation. An unmodeled tropospheric zenith delay error causes an error primarily in height determination. At very high elevation angles, an error in the tropospheric zenith delay is almost indistinguishable from the unmodeled height component. The zenith delay error can be well recovered at low elevation angles, which can subsequently increase the error in height determination if not done correctly. These results can be improved if tight constraints are placed on the station height components in static applications.

On the other hand, the adaptive estimator can be used in kinematic applications as well as static applications. The adaptive estimator captures the changes of satellite geometry and mapping functions over a relatively short time period. This ability of the adaptive estimator enables us to distinguish the tropospheric zenith delay from the unmodelled height component.

FIGURE 5 shows the wet zenith delay estimated at every epoch, without the assumption of atmospheric azimuthal asymmetry and use of gradient estimation. We can clearly see the effects of the forgetting factor α on the wet zenith delay estimates. When α = 1, we obtain noisy wet zenith delay estimates as no smoothing process works on the estimates. On the other hand, we will have a smoother wet zenith delay estimate when α becomes smaller.

The convergence patterns of positioning solutions (vertical component) are illustrated in **FIGURE 6**. We determined the reference solutions by least-squares estimation after removing the atmospheric delays and ambiguities that can be estimated by fixing the coordinates of the two reference stations, CGSJ and DRHS. Normally, a better performance of the adaptive estimator is anticipated for a smaller forgetting factor (that is, a longer smoothing time interval) under typical atmospheric conditions. However,

▲ **FIGURE 7** Convergence test of positioning solutions when α = 0.001 and no gradients were estimated.

▲ **FIGURE 8** Convergence test of positioning solutions when α = 0.001 and no gradients were estimated.

its performance may not be the same under severe atmospheric conditions. **FIGURE 7** illustrates how well positioning solutions converge to the reference solutions when α = 0.001.

We also tried to estimate the tropospheric delays with atmospheric gradients and azimuthal asymmetry. In this case, the tropospheric parameter vector includes the wet zenith delay, D_{wz}, and the horizontal (north, G_N, and east, G_E) delay gradients. The zenith wet delay and the north delay gradient did not converge for a relatively long time period. It took about fifty minutes before they converged. Furthermore, as illustrated in **FIGURE 8**, positioning solutions were biased with respect to the reference solutions. The horizontal components (especially, the north solution) were more significantly biased than the vertical components.

The poor performance with atmospheric gradients and azimuthal asymmetry, for both the single epoch observation model and the adaptive estimator, resulted from the fact that the tropospheric parameters are almost indistinguishable from the unmodelled position components in this case. To improve its performance, we may need a longer smoothing time interval or more

satellites at lower elevation angles. Unfortunately, this may not always be practical for real-time applications.

Static Results. A total of three permanent stations already in operation have been used to compute the geodetic coordinates of CGSJ and DRHS. One station is located in Fredericton, New Brunswick: the IGS station UNB1 (now UNBJ) on the UNB Fredericton campus. The other two stations

	Mean (cm)	Std. (cm)	r.m.s. (cm)
dX	-0.1	1.1	1.1
dY	-0.2	2.3	2.3
dZ	-0.3	1.5	1.5
dN	0.5	1.4	1.5
dE	0.6	1.3	1.4
dU	0.4	2.3	2.3

▲ **TABLE 1** Summary statistics for ambiguity-fixed RTK solutions, CGSJ to DRHS

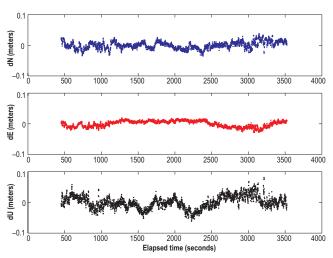|	Mean (cm)	Std. (cm)	r.m.s. (cm)
dX	-0.1	0.9	0.9
dY	-0.2	1.7	1.7
dZ	-0.3	1.6	1.6
dN	-0.3	1.2	1.2
dE	-0.2	1.0	1.0
dU	-0.1	2.0	2.0

▲ **TABLE 2** Summary statistics for differences between ambiguity fixed RTK solutions: CGSJ to BOAT and DRHS to BOAT

are the U.S. Continuously Operating Reference Station ESPT, in Eastport, Maine, run by NOAA, and the IGS station HLFX, in Halifax, run by Natural Resources Canada. Seven days of raw GPS data from each of the five reference stations were processed with the Bernese V4.2 software. During the processing, the IGS final SP3 orbit product was used and the coordinates of all three permanent stations were held fixed to their published ITRF00 coordinates to estimate the coordinates of CGSJ and DRHS. The formal estimated uncertainty of these coordinates was smaller than 2 millimeters.

The first step in the RTK processing to validate the success of our approach was a confirmation of the RTK positioning solutions using the data recorded at CGSJ and DRHS. In this case, although test data was recorded in static mode, the data was processed as if it was obtained in kinematic mode. CGSJ was treated as the base station and DRHS as the rover. We present the statistics for the ambiguity-fixed RTK positioning solutions between CGSJ and DRHS in **TABLE 1**.

Kinematic Results. Since we have validated the success of the ionosphere-nullification approach using the data recorded in static mode at CGSJ and DRHS, we further tried to confirm its validity using the data collected in kinematic mode with the onboard GPS receiver. A pair of long/short baselines (DRHS to BOAT and CGSJ to BOAT) was estimated at each epoch and used to characterize long-baseline positioning performance.

After a pair of long/short baselines was estimated at each epoch, baseline components were compared for each pair of solutions. As **FIGURE 9** shows, the long and short RTK positioning solutions vary by only a few centimeters. **TABLE 2** provides the summary statistics. Mean differences of a few millimeters are observed in each Cartesian component, and the comparison one-sigma noise

▲ **FIGURE 9** Difference of RTK positioning solutions, CGSJ to BOAT (short baseline) and DRHS to BOAT (long baseline) in local geodetic coordinates

level is at the few-centimeter level.

Conclusions

We have experienced a number of challenges in resolving ambiguities for longer baselines. One of the major challenges is the presence of unmodeled atmospheric delays. In this article, we discussed a possible new approach that does not rely on the convergence of a parameter (atmospheric delay or float ambiguity), but which nullifies and estimates the effect of the differential atmospheric delay in the ambiguity search process.

We propose the use of the ionosphere-nullification technique, which can virtually eliminate the large first-order ionospheric effects using the ionosphere observable in the simultaneous ambiguity search process. We also propose use of the adaptive estimator for estimating the tropospheric delays.

Although this technique was originally developed for single-baseline RTK over long distances in kinematic mode, it can be considered as an alternative approach or a parallel process for network RTK when requiring extrapolation of the differential ionospheric corrections for a rover located outside the network. It can also be used in cases where a rover located inside the network is experiencing localized anomalous ionospheric delays due to severe ionospheric activity. We plan to implement this technique in our network RTK software, which is currently under development.

Acknowledgments

Manufacturers

The reference stations and ferry were equipped with **NovAtel** *(www.novatel.com)* DL-4 receivers and GPS-600 antennas.

DON KIM is a senior research associate in the Department of Geodesy and Geomatics Engineering at UNB. He has a bachelor's degree in urban engineering, and an M.Sc.E. and Ph.D. in geomatics from Seoul National University. He has been involved in GPS research since 1991 and active in the development of an ultra high-performance RTK system. He received the Dr. Samuel M. Burka Award for 2003 from ION.

FURTHER READING

■ **Real-time Kinematic (RTK) Positioning**

"Ubiquitous Positioning: Anyone, Anything; Anytime, Anywhere" by X. Meng, A. Dodson, T. Moore, and G. Roberts in *GPS World*, Vol. 18, No. 6, June 2007, pp. 60–65.

"Network RTK: Getting Ready for GNSS Modernization" by H. Landau, X. Chen, A. Kipka, and U. Vollath in *GPS World*, Vol. 18, No. 4, April 2007, pp. 50–55.

"RTK GPS" by R.B. Langley in *GPS World*, Vol. 9, No. 9, September 1998, pp. 70–76.

■ **Fast Ambiguity Resolution**

"Towards Instantaneous RTK GPS over 100 km Distances" by I. Kashani, D. Grejner-Brzezinska, and P. Wielgosz in *Proceedings of The Institute of Navigation 60th Annual Meeting*, Dayton, Ohio, June 7–9, 2004, pp. 679–685.

"Fast GPS Ambiguity Resolution On-the-fly for Real-time Application" by H.-J. Euler, and H. Landau in *Proceedings of the 6th International Geodetic Symposium on Satellite Positioning*, Columbus, Ohio, March 17-20, 1992, pp. 650–659.

■ **Handling Ionospheric Effects**

"Ionosphere-Nullification Technique for Long-Baseline Real-Time Kinematic Applications" by D. Kim and R.B. Langley in *Navigation: Journal of The Institute of Navigation*, Vol. 54, No. 3, Fall 2007, pp. 227–240.

"Ionospheric Modeling: The Key to GNSS Ambiguity Resolution" by T. Richert and N. El-Sheimy in *GPS World*, Vol. 16, No. 6, June 2005, pp. 35–40.

Fast Precise GPS Positioning in the Presence of Ionospheric Delays by D. Odijk, Ph.D. dissertation, Dept. of Mathematical Geodesy and Positioning, Delft University of Technology, Delft University Press, Delft, The Netherlands, 2002.

■ **Handling Tropospheric Effects**

"Performance of Long-baseline Real-time Kinematic Applications by Improving Tropospheric Delay Modeling by D. Kim, S. Bisnath, R.B. Langley, and P. Dare in *Proceedings of ION GNSS 2004*, the 17th International Technical Meeting of The Institute of Navigation, Long Beach, California, September 21-24, 2004, pp. 1414–1422.

"Effects of Atmospheric Azimuthal Asymmetry on the Analysis of Space Geodetic Data" by G. Chen and T.A. Herring in *Journal of Geophysical Research*, Vol. 102, No. B9, 1997, pp. 20489-20502.